

Cold Fermi atomic gases in a pumped optical resonator

Jonas Larson^{1,2}, Giovanna Morigi³ and Maciej Lewenstein^{1,4}

¹*ICFO–Institut de Ciències Fotòniques, E-08860 Castelldefels, Spain*

²*NORDITA, 106 91 Stockholm, Sweden*

³*Departament de Física, Universitat Autònoma de Barcelona, E-08193 Bellaterra, Spain and*

⁴*ICREA– Institució Catalana de Recerca i Estudis Avançats, E-08010 Barcelona, Spain*

(Dated: November 8, 2018)

We study systems of fully polarized ultracold atomic gases obeying Fermi statistics. The atomic transition interacts dispersively with a mode of a standing-wave cavity, which is coherently pumped by a laser. In this setup, the intensity of the intracavity field is determined by the refractive index of the atomic medium, and thus by the atomic density distribution. Vice versa, the density distribution of the atom is determined by the cavity field potential, whose depth is proportional to the intracavity field amplitude. In this work we show that this nonlinearity leads to an instability in the intracavity intensity that differs substantially from dispersive optical bistability, as this effect is already present in the regime, where the atomic dipole is proportional to the cavity field. Such instability is driven by the matter waves fluctuations and exhibits a peculiar dependence on the fluctuations in the atomic density distribution.

PACS numbers: 42.50.Pq, 42.50.Nn, 42.50.Wk, 71.10.Fd

I. INTRODUCTION

Cavity Quantum Electrodynamics (CQED) is one of the most rapidly developing areas of modern quantum optics and atomic molecular, and optical physics [1, 2]. In its early days optical instabilities, with the paradigm example of optical bistability were in the center of interest [3, 4]. Optical bistability emerges from the nonlinear response of the dipolar transitions of atoms to the cavity field, to which they couple. Theoretically, such dynamics are well described by mean field theories formulated for macroscopic variables, such as the cavity field intensity and the total atomic polarization [5, 6, 7]. Fluctuations of the polarization, in particular in the quantum regime, may play an important role in these processes, as pointed out for instance in the seminal studies of the late Dan Walls and collaborators (see [1] and references therein). Typically, however, these dynamics are characterized by few *macroscopic* quantum degrees of freedom, where quantum fluctuations are small, except at the instability points. Nonlinearity at the microscopic level has since then been reached by high-finesse resonators, where the strong coupling regime between a single atom and a single photon have been realized in several milestones experiments [8, 9, 10]. In this regime the quantum dynamics of few *microscopic* quantum degrees of freedom dominates the behavior of the system, and quantum fluctuations are typically large.

Recently experimental progress has allowed one to strongly couple cold atomic gases with the electromagnetic field mode of a resonator. This line of research, which we would like to term cavity QED of many-body systems, was stimulated by the observation on the interdependence between intracavity field and atomic motion via of the mechanical effects of light [11, 12]. This was confirmed by seminal experiments, which demonstrated cavity cooling of atoms [13] and selforganization of atoms

in regular patterns inside pumped cavities [14, 15]. Most recently, the coherent coupling between a Bose-Einstein condensate and a cavity field has been experimentally demonstrated [16, 17, 18]. Moreover, the nonlinear interaction between ultracold atoms and the field of a cavity mode had been experimentally observed [19]. In this new ultracold regime, theoretical work on bosonic atomic gases showed that the matter-wave quantum fluctuations and the spatial mode variance give rise to additional nonlinear atom-field effects [20], leading to features of the phase diagram which suggest novel bistability phenomena [21, 22, 23].

In this work, we consider a gas of ultracold and polarized fermionic atoms, whose dipolar transition interacts dispersively with the mode of a standing-wave resonator. In the regime in which the atomic polarization is linear in the field amplitude, and hence where there is no usual optical bistability, we encounter instabilities of the intracavity field which originate from the coupling with the atomic motion. The theoretical model we apply is based on a second-quantized approach for the description of the atomic and of the field degrees of freedom, in the regime in which the atomic internal degrees of freedom are eliminated from the equations in second order perturbation theory. These dynamics are studied by numerically integrating the Heisenberg equations of motion. The results show that the instabilities of the intracavity field intensity are driven by the pump strength and by the atomic density, and indirectly depend on the degree of localization of the atoms at the minima of the cavity potential.

This article is organized as follows. In Section II we theoretically derive the model, in Sec. III we solve numerically the coupled Heisenberg equations of motion for field and atoms for a fixed number of atoms and thoroughly discuss the validity of the considered approximations and experimental parameters. The conclusions and outlook are presented in Sec. IV.

II. THEORETICAL DERIVATION OF THE MODEL

In this section we derive the theoretical model, which is at the basis of the studies presented in Sec. III. In order to introduce the many-body theory, which is the starting point of our study, let us first review the Hamiltonian of a single two-level atom of mass m interacting with a cavity field which is pumped coherently by an external, monochromatic field. We denote by $\hat{\sigma} = |g\rangle\langle e|$ and $\hat{\sigma}^\dagger$ the atomic lowering and raising operators of the dipole transition at frequency ω_a with ground and excited states $|g\rangle, |e\rangle$, and by \hat{a} and \hat{a}^\dagger the annihilation and creation operators of a cavity photon at energy $\hbar\omega_c$. We further assume that the atomic motion is along the cavity axis X , while the radial degrees of freedom are frozen out, and denote by the operators \hat{P} and \hat{X} the atomic centre-of-mass momentum and position. In the dipole and rotating wave approximation, the Schrödinger equation of atomic and cavity degrees of freedom is governed by the Hamiltonian [21]

$$H_{JC} = \frac{\hat{P}^2}{2m} - \hbar\tilde{\Delta}_a\hat{\sigma}^\dagger\hat{\sigma} - \hbar\tilde{\Delta}_c\hat{a}^\dagger\hat{a} - i\hbar g(\hat{X})(\hat{\sigma}^\dagger\hat{a} - \hat{a}^\dagger\hat{\sigma}) - i\hbar\tilde{\eta}(\hat{a} - \hat{a}^\dagger). \quad (1)$$

which is here given in the reference frame rotating at the pump frequency ω_p . The parameters $\tilde{\Delta}_a = \omega_p - \omega_a$ and $\tilde{\Delta}_c = \omega_p - \omega_c$ are the detunings of the pump from atomic and cavity mode frequencies, respectively, and $\tilde{\eta}$ is the pump amplitude. The dipole-cavity mode coupling has position-dependent strength $g(\hat{X}) = g_0 \cos(q\hat{X})$ with q the cavity-mode wave number. For large detuning $|\tilde{\Delta}_a|$ the internal atomic level can be eliminated from the equations of cavity and atomic external degrees of freedom [22]. The effective Hamiltonian reads

$$H = \frac{\hat{P}^2}{2m} + \hbar\tilde{U}_0\hat{a}^\dagger\hat{a}\cos^2(q\hat{X}) - \hbar\tilde{\Delta}_c\hat{a}^\dagger\hat{a} - i\hbar\tilde{\eta}(\hat{a} - \hat{a}^\dagger), \quad (2)$$

with $\tilde{U}_0 = g_0^2/\tilde{\Delta}_a$, and where we have considered temperatures for which the atomic motion is frozen on the time scale in which the internal degrees of freedom appreciably evolve.

For later convenience we introduce the dimensionless variables

$$\hat{p} = \frac{\hat{P}}{\hbar q}, \quad \hat{x} = q\hat{X}, \quad t = \tilde{t}\omega_r, \quad (3)$$

$$U_0 = \frac{\tilde{U}_0}{\omega_r}, \quad \Delta_c = \frac{\tilde{\Delta}_c}{\omega_r}, \quad \eta = \frac{\tilde{\eta}}{\omega_r}.$$

where $\omega_r = \frac{\hbar q^2}{2m}$ is the recoil frequency.

We remark that when neglecting the coupling between cavity and motion, hence in the classical limit, Hamiltonian in Eq. (2) does not give rise to instabilities like in

optical bistability. Dispersive optical bistability, in fact, would appear when the next order in the perturbative expansion is included, giving rise to a nonlinear (Kerr) term of the form $\hat{a}^\dagger\hat{a}^\dagger\hat{a}\hat{a}$ [24, 25]. In this work we deal with the parameter ranges in which such Kerr nonlinearity can be neglected, and hence classical optical bistability does not appear. Moreover, we consider the regime in which the mechanical effects of photon-atom interactions are relevant. In this range, the nonlinearity in the dynamics of Hamiltonian (2) is solely due to the coupling between the cavity field and the atomic quantum center-of-mass variables.

A. Many-body Hamiltonian

We now introduce the system which we investigate in this paper, namely a gas of N fully polarized fermionic atoms interacting dispersively with the mode of the resonator. Denoting by $\hat{\Psi}(x)$ the atomic field operators obeying Fermi commutation rules, the rescaled Hamiltonian in second quantization reads

$$H - \Delta_c\hat{a}^\dagger\hat{a} - i\eta(\hat{a} - \hat{a}^\dagger) + \int dx \left(-\hat{\Psi}^\dagger(x)\frac{d^2}{dx^2}\hat{\Psi}(x) + U_0\cos^2(x)\hat{a}^\dagger\hat{\Psi}^\dagger(x)\hat{\Psi}(x)\hat{a} \right), \quad (4)$$

where we have taken care of the proper ordering between atomic and field operators, which is here normal (see also [22]).

Let us now consider that the number of photons is fixed to the value n . Then, after tracing out the photonic degrees of freedom from Hamiltonian (4), the resulting Hamiltonian describes the motion of N Fermions in the optical lattice of the cavity field, whose depth is proportional to the number of photons n . Hence, the degree of localization of the atoms at the minima of the potential wells depends on n , and so will the Wannier functions in the tight-binding limit. We now assume that the atoms are well localized at the minima of the potential, and expand the atomic field operators in the tight-binding limit [26] in the corresponding Wannier functions for the lowest Bloch band,

$$\hat{\Psi}(x) = \sum_{i=1}^K \hat{f}_i w_{\hat{n}}(x - x_i) \quad (5)$$

where \hat{f}_i is the annihilation operator of a fermion at site i , $w_{\hat{n}}(x - x_i)$ is the Wannier function localized at site i , and K is the number of lattice sites. The subscript \hat{n} indicates the operator valued dependence of the Wannier functions on the number of photons $\hat{n} = \hat{a}^\dagger\hat{a}$. Such an expansion, considering only the lowest band, is known to be justified for large or moderate lattice depths, which we will discuss in more detail later on. Using the Wannier expansion within the single-band approximation, Eq. (5),

we obtain from Eq. (4) the Hamiltonian

$$\mathcal{H} = \sum_{i,j=1}^K [E_{ij}(\hat{n}) + U_0 (\hat{a}^\dagger J_{ij}(\hat{n}) \hat{a})] \hat{f}_i^\dagger \hat{f}_j - \Delta_c \hat{a}^\dagger \hat{a} - i\eta (\hat{a} - \hat{a}^\dagger) \quad (6)$$

where

$$E_{ij}(\hat{n}) = \int dx w_{\hat{n}}^*(x-x_i) \left(-\frac{d^2}{dx^2} \right) w_{\hat{n}}(x-x_j), \quad (7)$$

$$J_{ij}(\hat{n}) = \int dx w_{\hat{n}}^*(x-x_i) \cos^2(x) w_{\hat{n}}(x-x_j),$$

are the coupling parameters which depend on the number of photons of the cavity field. In the tight-binding approximation we keep only on-site and nearest-neighbour interactions in Eq. (6), and denote the relevant coupling parameters by $E \equiv E_{ii}$, $J \equiv J_{ii}$, $E_1 \equiv E_{i,i+1}$, and $J_1 \equiv J_{i,i+1}$. This is legitimate in the single band regime. We impose periodic boundary conditions and use the representation $\hat{c}_k = \sum_j \hat{f}_j e^{ikj}$, where \hat{c}_k (\hat{c}_k^\dagger) annihilates (creates) a fermion at the rescaled quasi-momentum k , with k in the interval $[-1, 1]$ and step $\delta k = 2/K$. In this representation, the number operator $\hat{N} = \sum_j \hat{f}_j^\dagger \hat{f}_j$ and the hopping operator $\hat{B} = \sum_j \hat{f}_j^\dagger \hat{f}_{j+1} + \text{H.c.}$ get the diagonal forms

$$\hat{N} = \sum_k \hat{c}_k^\dagger \hat{c}_k, \quad (8)$$

$$\hat{B} = 2 \sum_k \cos(k\pi) \hat{c}_k^\dagger \hat{c}_k,$$

Hence, the new Hamiltonian takes the form

$$\mathcal{H} = -\Delta_c \hat{a}^\dagger \hat{a} - i\eta (\hat{a} - \hat{a}^\dagger) + \mathcal{H}_1(\hat{n}) + \mathcal{H}_2(\hat{n}) \hat{a}^\dagger \hat{a} \quad (9)$$

with

$$\mathcal{H}_1(\hat{n}) = \sum_k \left[E + 2E_1 \cos(k\pi) \right] \hat{c}_k^\dagger \hat{c}_k,$$

$$\mathcal{H}_2(\hat{n}) = U_0 \sum_k \left[J(\hat{n}-1) + J_1(\hat{n}-1) 2 \cos(k\pi) \right] \hat{c}_k^\dagger \hat{c}_k. \quad (10)$$

Here, we used the relation $\mathcal{F}(\hat{n}) \hat{a} = \hat{a} \mathcal{F}(\hat{n}-1)$ for any function $\mathcal{F}(z)$ which is analytic in the scalar variable z .

B. Nonlinearities in the coupling parameters

Equation (9) describes dynamics, which couple in a nonlinear way cavity and atomic degrees of freedom. In particular, the coupling parameters E , E_1 , J , J_1 depend on the number of photons, since they are integrals of Wannier functions, which themselves depend on the intensity of the cavity field. In order to better understand

the character of this dependence on the intracavity photon number we evaluate their explicit form by replacing the Wannier functions in Eqs. (7) by Gaussians functions,

$$w_{\hat{n}}(x-x_i) \approx w_{\hat{n}}^G(x-x_i) = \frac{1}{\sqrt{\pi\sigma^2}} e^{-\frac{(x-x_i)^2}{2\sigma^2}}, \quad (11)$$

where $\sigma = |V|^{-1/2}$ and $V = U_0 n$ is the potential depth at a fixed number of photons n . Moreover, we modify the Gaussian functions by imposing the condition $\int dx w_{\hat{n}}^G(x-x_i) w_{\hat{n}}^G(x-x_j) = \delta_{ij}$, which allows us to avoid non-physical contributions. This ansatz is usually valid within the tight-binding approximation as will be further discussed in Sec. III D and has been checked in [22]. Using these modified Gaussian functions we solve the integrals in Eq. (7) and obtain

$$E = \frac{1}{y},$$

$$J = \frac{1}{2} (1 - se^{-y}), \quad (12)$$

$$E_1 = -\frac{1}{2y^2} e^{-\frac{\pi^2}{4y}} (2y + \pi^2),$$

$$J_1 = s \frac{1}{2} e^{-\frac{\pi^2}{4y}} e^{-y},$$

where we have introduced $y = \sigma^2 = |V|^{-1/2}$ and $s = \text{sign}(\Delta_c)$. Relaxing the orthogonality condition one would find that the amplitude $|J_1|$ is different for red or blue detuning. The sign dependence s in J and J_1 arises from the fact that the Wannier functions are centered at different positions in the two cases. From these expressions we find $|J_1| < 18J$ within the validity of the tight-binding approximation, which according to Ref. [22] is given by $y < 0.5 - 1$. Moreover, the contribution from ℓ -neighbours can be estimated to be $|J_\ell/J_1| = \exp[-(\ell^2 - 1)\frac{\pi^2}{4y}] \ll 1$, which justifies neglecting next nearest-neighbour terms and so forth in Eqs. (9).

III. DYNAMICS AND STEADY STATE OF THE CAVITY FIELD

In this section we study analytically and numerically the dynamics and steady state of the cavity field, focussing on instabilities due to the interplay between field and matter wave fluctuations at a fixed number of atoms N . We consider the Heisenberg equations of motion for the field operators,

$$\dot{\hat{a}} = -i[\hat{a}, \mathcal{H}_1(\hat{n})] - i[\hat{a}, \mathcal{H}_2(\hat{n})] \hat{n} - i\mathcal{H}_2(\hat{n}) \hat{a} + i\Delta_c \hat{a} - \kappa \hat{a} + \eta + \hat{\xi}_a, \quad (13)$$

$$\dot{\hat{n}} = \eta (\hat{a} + \hat{a}^\dagger) - 2\kappa \hat{n} + \hat{\xi}_n, \quad (14)$$

and similarly for \hat{a}^\dagger . These are coupled to the equations for the atomic field operators, and where $\hat{\xi}_i$ are

the quantum noise operators, such that $\langle \hat{\xi}_i(t) \rangle = 0$ and $\langle \hat{\xi}_i(t) \hat{\xi}_i^\dagger(t') \rangle = 2\kappa\delta(t-t')$ for $i = a, n$. Such fluctuations vary on time scales which are faster than $1/\kappa$, and will be neglected when taking the mean values on the coarse-grained time scales, at which we analyze the dynamics in what follows. The numerics are carried out by first evaluating the commutators and then replacing the operators by c -numbers, $\hat{a} \rightarrow \alpha$, $\hat{a}^\dagger \rightarrow \alpha^*$ and $\hat{n} \rightarrow \bar{n} = |\alpha|^2$, and then solving the differential equations using the regular Runge-Kutta method. As initial conditions we thus use $\bar{n}(t=0) = n_0$, $\bar{a} = \sqrt{n_0}$ and $\bar{a}^* = \sqrt{n_0}$ for some real n_0 . Note that the commutators are carried out exactly, *i.e.* $[\hat{a}, g(\hat{n})] = \hat{a}(g(\hat{n}) - g(\hat{n}-1))$, and the c -number replacement is done afterwards. Truncating the system dynamics to only three equations and dropping the operator structure should be justified for the open system we consider.

A. Intracavity field intensity

The intracavity intensity is found from the mean value of photons,

$$\bar{n}(t) = \langle \hat{n}(t) \rangle. \quad (15)$$

This average is taken over field and atomic degrees of freedom, assuming that the cavity field variables relax to a stationary value on a faster time scale than the time scale of the evolution of the atomic variables, hence for $\kappa \gg k_B T/\hbar$, with κ the cavity decay rate, k_B Boltzmann's constant and T the temperature. In this regime, a closed expression for the photon number operator can be found in the limit in which the number of photons is sufficiently large (In fact, the analytic expression gives to a good approximation also the steady state solution for weak fields.). In this regime we approximate

$$\mathcal{F}_2(\hat{n}-1) \approx \mathcal{F}_2(\hat{n}) - \partial \mathcal{F}_2'(\hat{n}), \quad (16)$$

where \mathcal{F} is any analytical function and ∂ indicates derivative with respect to photon number, and from Eq. (10) we find

$$\mathcal{H}_2(\hat{n}) \approx U_0 \sum_k \left[(J - \partial J) + (J_1 - \partial J_1) 2 \cos(k\pi) \right] \hat{c}_k^\dagger \hat{c}_k. \quad (17)$$

Using similar relations for the commutators in Eq. (14), we find an analytical expression that the mean photon number has to fulfill,

$$\bar{n} = \frac{\eta^2}{\kappa^2 + (\Delta_c - \xi(\bar{n}))^2} \quad (18)$$

where

$$\xi(\hat{n}) = \mathcal{H}_2 + \partial \mathcal{H}_2 + \partial \mathcal{H}_1 + \partial \mathcal{H}_2 \hat{n}. \quad (19)$$

In order to evaluate Eq. (15) we assume that the atomic state is the ground state of the potential, whose depth

is determined by the time-dependent number of photons $\bar{n}(t)$. The ground state is then evaluated assuming that the tight-binding and the single-band approximations are valid during the evolution of the field. This treatment is hence valid in specific parameter regimes, namely when the rate of variation of the photon number, giving the height of the cavity potential, remains smaller than the energy gap between the lowest and the first band, and when the mean number of photons \bar{n} warrants sufficient localization of the atoms, according to the relation

$$y = \frac{1}{\sqrt{|U_0| \bar{n}}} \ll 1.$$

We have numerically checked that for $y < 0.5$ (which coincides with the tight-binding and Gaussian approximations), the first band gap is larger than the recoil energy. Thus, remaining in the validity regimes for the tight-binding and Gaussian approximations ($y < 0.5$), also warrants no non-adiabatic coupling of excited bands. Further, the large band gap makes the system resistant to nonzero temperature excitations.

B. Many-body atomic state

In order to calculate any quantities we need to specify the particular state of the atoms. In the regime in which we can assume that the cavity field variables relax to a stationary value on a faster time scale than the time scale of the evolution of the atomic variables, we can eliminate the photon variables from the atomic Heisenberg equations. In doing this we follow the procedure discussed in [22], now applied to fermionic atoms. Hence finding that the atomic dynamics are determined by an effective Hamiltonian of the form

$$\mathcal{H}_{\text{eff}} = E\hat{N} + f(\hat{N}) + \left[E_1 + \frac{U_0 \eta^2 J_1}{\kappa^2 + \zeta^2(\hat{N})} \right] \hat{B}, \quad (20)$$

where

$$f(\hat{N}) = \frac{\eta^2}{\kappa} \arctan \left[\frac{\zeta(\hat{N})}{\kappa} \right], \quad (21)$$

$$\zeta(\hat{N}) = \Delta_c - U_0 J_0 \hat{N}$$

and the coupling terms given in (12). This Hamiltonian is derived at leading order in an expansion in $1/N$, assuming a scaling such that the number of lattice sites K is proportional to the number of atoms N where we assume a fixed number of atoms N . The coefficients of this Hamiltonian depend on the atomic variables through the nonlinear coupling with the cavity field [21, 22]. When they are independent of the atomic variables, for instance in the case of Fermi gases in deep optical lattices in free space, the ground state of this Hamiltonian is the usual Fermi sea, where the value $\sum_{i=1}^N |k_i|$ is minimized. Thus,

the many body ground state is found by filling with one atom all states with quasi-momentum k up to the Fermi quasi-momentum k_F , assuming that k_F is smaller than the edge of the Brillouin zone. This simple procedure cannot be applied when the nonlinearity in the Hamiltonian gives dispersion curves that may exhibit local minima, which can be at values of k different from $k = 0$ (at the center of the Brillouin zone). Finding the distribution that gives the smallest energy is in general a linear programming (LP) optimization problem with two constraints: (i) at most one particle can occupy each site and (ii) the total number of particles equals N . However, since the number of particles per site is a discrete variable, $n_i = 0, 1$, standard LP techniques are not applicable. We use instead a variational approach where we assume that the usual Fermi sea is the ground state, and check its stability against perturbations. Such check is made by randomly extracting a single fermion from the Fermi sea and putting it in a random state outside the sea. We then compare the energies, calculated using \mathcal{H}_{eff} in Eq. (20), for the Fermi sea and the perturbed state. Repeating this procedure sufficiently many times, we find that the energy of the Fermi sea (according to our ansatz) is usually lower than the perturbed one. In some cases, however, the perturbed state is energetically favorable. On the other hand, the difference in energy between the two states is extremely small for the parameter regimes of interest and hence does not affect the general structure of our results. We have also compared the energy of a fully random distribution with the one of the Fermi sea and in all examples we considered found the usual Fermi sea to have a lower energy. Still, these situations are potentially of great interest, since they may indicate novel quantum phase transitions due to the change of geometry, or even topology of the Fermi surface, similar to what happens in graphene (cf. [27, 28]). These questions go beyond the focus of the present paper, and will be studied elsewhere.

C. Quantum optical bistability

We now evaluate Eq. (15) assuming that the atoms are in the state described by the usual Fermi sea, and find a nonlinear equation for \bar{n} , which may exhibit multiple solutions. We remind that such nonlinearity is not due to the nonlinear coupling between atomic dipoles and fields, but instead originates from the quantum fluctuations of the atoms at the minima of the confining potential. In order to highlight this behaviour, we express $\bar{n} = 1/U_0 y^2$, using the relation between the depth of the potential and the width of the Gaussian functions. From Eq. (15), using the approximation $[\hat{a}, g(\hat{n})] \approx \frac{\partial g(\hat{n})}{\partial \hat{n}} \hat{a} \equiv \partial g(\hat{n}) \hat{a}$ in Eq. (19), we find the nonlinear equation which determines y ,

$$|U_0| \eta^2 y^2 - \kappa \left\{ \Delta_c - \frac{U_0 N}{2} \left(f_1(y) + \tilde{B} e^{-\frac{\pi^2}{4y}} f_2(y) \right) \right\}^2 \quad (22)$$

where $\tilde{B} = 2 \sum_{i=1}^N \cos(k_i \pi) / N$ is the mean value of the operator $\langle B \rangle / N$, taken on the Fermi sea of atoms, and

$$f_1(y) = 1 + sy - se^{-y}(1 + y/2) \quad (23)$$

$$f_2(y) = se^{-y} \left(1 + \frac{y}{2} - \frac{\pi^2}{8y} \right) + \frac{\pi^4}{8y} - \frac{6\pi^2}{8} - y. \quad (24)$$

Here we neglected small terms such as the derivative of the E_1, J_1 -terms, which indeed has been verified to only give minimal corrections.

Figure 1 displays the set of values (\bar{n}, N) for which Eq. (22) is satisfied. The parameter regime is restricted to $y < 0.5$, where our treatment is valid. In particular, in Fig. 1 (a) the detuning $\Delta_a > 0$ and the atoms are trapped at the nodes of the cavity potential, where for maximum localization, $y \rightarrow 0$, the coupling with the resonator vanishes. Nonlinearity here arises due to the finite size of the fluctuations. In Fig. 1(b), instead, $\Delta_a < 0$, and the atoms are confined at the antinodes, where the coupling to the field is maximum. For large atom numbers the effect of small position fluctuations at these points gives a small correction to the cavity intensity, and the system shows less sensitivity on the external parameters, see also [21, 22].

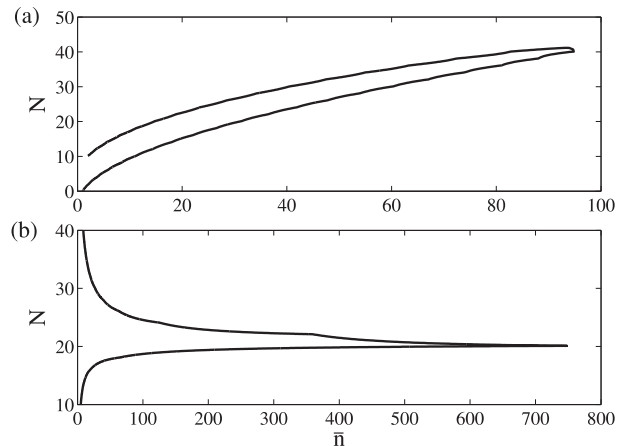


FIG. 1: Set of parameters (\bar{n}, N) for which Eq. (22) is satisfied. The dimensionless parameters are $\kappa = 1$, and (a): $U_0 = 10$, $\eta = 10$, $\Delta_c = 10$ and (b): $U_0 = -1$, $\eta = 30$, $\Delta_c = -20$. In both plots we assumed $K = 50$ sites of the cavity potential. The curves are shown for the values of (\bar{n}, N) such that $y < 0.5$, when the tight-binding approximation is valid.

In order to check the stability of the solutions, we numerically solve the Heisenberg equations in Eqs. (13)-(14) for various initial values of \bar{n} at a fixed number of atoms N , as previously explained. Figure 2 displays the evolution of some different values of the mean number of photons $\bar{n}(t)$. In particular, Figs. 2(a)-(c) have been evaluated in the same parameter regime of Fig. 1(a) and for a particular choice of the number of atoms N . In Fig. 2 (a) and (b) it is visible that the mean value exhibits two possible asymptotic solutions, which depend

on the initial value, while in Fig. 2 (c) there is only one asymptotic value of \bar{n} . Comparing with the results in Fig. 1(a), we find that only the solutions of the lower branch of the curve (\bar{n}, N) in that figure are recovered, while the upper branch is unstable. The additional solutions with small asymptotic \bar{n} in fig. 2 (a) and (b) correspond to $y > 0.5$ and are thus beyond the validity regime of our approximations and hence not visible in Fig. 1 (a). The lower two plots, Figs. 2(d) and (e), should be compared with Fig. 1(b). Here, one can observe that a small change in atomic number, $N = 20$ or $N = 18$, results in intracavity field intensities differing by a factor of about 100. We again pointed out that by calculating the Heisenberg equations of motion we use the exact relation $[\hat{a}, g(\hat{n})] = (g(\hat{n}) - g(\hat{n} - 1))\hat{a}$, and do not impose any approximations involving derivatives as in (16). Still, the asymptotic solutions of the numerical integration agree well with the ones obtained from (22), which verifies the trustworthiness of the steady state results (22).

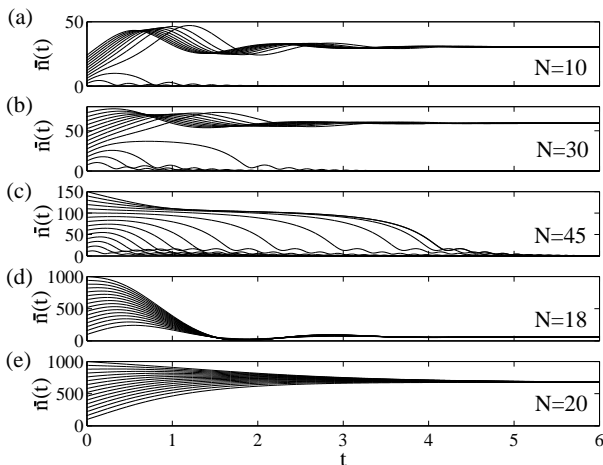


FIG. 2: Mean number of photons \bar{n} as a function of time, obtained by numerically integrating the Heisenberg equations in Eqs. (13)-(14) for different initial values $n(0)$ and for a fixed number of fermionic atoms N . In (a)-(c) the parameters correspond to the ones of Fig. 1(a), in (d),(e) to the ones of Fig. 1(b). In the calculations we assumed that the atoms are in the ground state of the cavity potential, and that the tight-binding regime and the single-band approximation are valid. This is fulfilled for $\bar{n} > 0.4$ in (a)-(c), and for $\bar{n} > 4$ in (d),(e). Once the curves reach below these limiting values, they lie outside the validity regime of our approximations.

We finally study the instability of the mean number of photons \bar{n} , and hence the cavity potential depth, as the pumping amplitude is varied. Typical examples are shown in Fig. 3, where the solutions for \bar{n}, N of Eq. (22) are plotted as a function of the pump amplitude η . The dashed middle branch represents an unstable solution of the equations. Note that the lower branch is almost identical to $\bar{n} = 0$. We see that \bar{n} exhibits jumps at critical values of the pump η , corresponding to an instability due to the nonlinear behaviour, to values in which

our approximations are invalid. Such regime is in the grey-shaded zone. Here, our treatment is invalid and we cannot make definite predictions. We conjecture that at these points the fermions are populating higher Bloch bands or forming a Fermi liquid. The study of this transition will be explored in detail in future works.

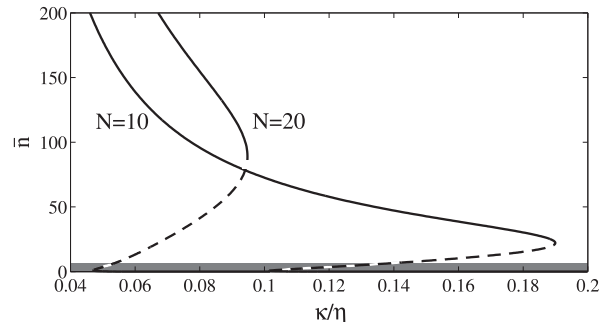


FIG. 3: Mean number of photons \bar{n} , evaluated in Eq.(22) for a fixed number of atoms $N = 10, 20$, as function of the pumping $1/\eta$ (in units of $1/\kappa$). The solid (dashed) line indicates the stable (unstable) solutions. The dimensionless parameters are $U_0 = 0.62$ and $\Delta_c = 5$, and the sites of the cavity potential are $K = 50$. The region shaded in grey corresponds to the values $\bar{n} < 7$ where the tight-binding and single-band approximations are not valid.

D. Validity of approximations and typical experimental parameters

Various approximations have been imposed throughout the paper and it is in order to summarize them and discuss their reliabilities. The very first assumption of our model system is the adiabatic elimination of the excited atomic levels and neglecting spontaneous emission. The justification of leaving out spontaneous emission, and at the same time taking into account for the cavity spectral line width and the single mode assumption, was discussed in detail in [22]. There we found effective atom-field couplings $g_0 \sim 2\pi \times 100$ MHz or $g_0 \sim 2\pi \times 700$ MHz using, respectively, the cavity decay rates κ of [17] or [18]. These are presently slightly outside the regime of experimental reach. This may, however, be circumvented by increasing the total number of atoms N [22]. To assure the elimination of the excited atomic state we should have $\Delta_a \sim 10g_0\sqrt{\bar{n}}$, where the average number of photons \bar{n} is typically 100. This suggests $U_0 < g_0$ and in our numerical analysis U_0 is of the same order as κ , while for realistic parameters one has $g_0 > \kappa$ and thus ensure that the upper atomic state can be eliminated.

We further imply the Gaussian, single band and tight-binding approximations in order to derive the many-body Hamiltonian (9). The validity of these approximations is thoroughly analyzed in [22] where it is found that they all break down for $y > 1$, or equivalently $|V| < 1$. In this work we consider $y < 0.5$ (or otherwise explicitly pointed

out) to meet this constrain. Especially, in the instability of field intensities as the pump amplitude is varied, shown in Fig. 3, are these approximations assumed to be violated. However, instability is still predicted, jumping from a strong cavity field to a weak one even if the true full state of the system cannot be predicted. Related is the conjecture of the Fermi sea state of the atoms. This requires an adiabatic change of any system parameters, but we have verified that our results are reproducible also for deviations from the Fermi sea state and therefore not restricted to the fully adiabatic limit. Consequently, the system is also robust against small but nonzero temperatures.

In solving for the dynamics, the set of Heisenberg equations of motion (13) and (14) is truncated to contain the equations for \hat{a} , \hat{a}^\dagger and \hat{n} , which is believed to be justified in the regime of fairly large cavity decay considered here. The analytical steady state result for the field amplitude uses $[\hat{a}, g(\hat{n})] \approx \partial g(\hat{n})\hat{a}$ and also neglects small terms in the final expression (22). This is supported since the results of the steady state numerical calculations of the Heisenberg equations coincide well with ones predicted by (22), even for small field amplitudes $\bar{n} < 10$.

To get an idea about characteristic experimental scales and quantities, we consider potassium atoms ^{40}K and a wave length $\lambda = 800$ nm, giving the recoil frequency $\omega_r \approx 50$ kHz. Thus, $t = 1$ corresponds to an unscaled time $\tilde{t} = 20$ μs , and estimating the critical temperature as $T = \hbar\omega_r/k_B$ one finds $T \sim 0.4$ μK . Note that cavity decay rates used in this paper are of order of the recoil frequency, i.e. realistic but rather small. However, we have verified that κ can be increased, while U_0 , η and Δ_c are scaled accordingly, and our results still remains.

IV. DISCUSSION AND CONCLUSIONS

We have reported on instability in the intracavity mean photon number, which are driven by the pump intensity and by the atomic density. Differing from usual optical bistability, these nonlinear effects arise in the regime in which the atomic polarization is linear in the intensity of the cavity field. In fact, such instability is due to nonlinear coupling between the atomic motion and the cavity field, whose dynamics and steady state depend in a complex way on various parameters, such as pump am-

plitude, frequency, and the atomic density distribution. The system we here consider is a gas of ultracold Fermi atoms, and the nonlinearity we observe is exclusively due to the coupling of the atoms with the resonator, whereby particle-particle collisions are neglected due to the Pauli principle. The atomic density distribution hence enters in determining the strength of the coupling of the atomic fermions to the cavity field, accordingly the height of the cavity potential which finally, closing this nonlinear circle, determines the atomic density distribution itself.

The dependence of the cavity field dynamics on the atomic density is indeed peculiar: At different atomic densities, different behaviours and instabilities of the cavity field are observed. One could hence conjecture that this system may also exhibit fluctuations and instabilities in the mean number of atoms, in the regime in which this is not fixed, as it could be observed when the gas is put in contact with a particle reservoir.

Further interesting outlooks emerge when considering the situation at larger intracavity intensities, in which the atomic polarization is nonlinear in the field. In this case, this nonlinearity, which corresponds to the one of dispersive optical bistability, adds to the one of the coupling to the motion, and gives rise to a competition between cavity potentials. In fact, at lower intensities the potential is of the form $\cos^2(\hat{X})$, while at larger fields it is a superposition of $\cos^2(\hat{X})$ and $\cos^4(\hat{X})$. Hence, instabilities in the atomic ground states may emerge, which are expected to give rise to novel behaviours. Such rich scenario is indeed exciting and requires different approaches to the study of this problem, which is under current investigation [29].

Acknowledgments

We thank Jakob Reichel, Stefan Ritter, and Mirta Rodriguez for helpful discussions. We acknowledge support of the Integrated Project "SCALA" of the European Commission (Contract No. 015714), the grants of the Spanish Ministerio de Educación y Ciencia (FIS 2005-04627; Consolider Ingenio 2010 "QOIT"; Ramon-y-Cajal; QNLP, FIS2007-66944), and the ESF-MEC Program "EUROQUAM" ("CMMC", "Fermix"). J.L. acknowledges support from the Swedish government/Vetenskapsrådet.

-
- [1] D. Walls and G. J. Milburn, *Quantum Optics*, (Springer, Berlin, 1994).
 - [2] P.R. Berman (Ed.) *Cavity Quantum Electrodynamics, Advances in Atomic, Molecular and Optical Physics, Supplement 2*, (Academic Pres, New York, 1994); S. M. Dutra, *Cavity Quantum Electrodynamics*, (Wiley-Interscience, Hoboken, 2004).
 - [3] H.M. Gibbs, S.L. McCall, and T.N.C. Venkatesan, *Phys. Rev. Lett.* **36**, 1135 (1976); H.M. Gibbs, F.A. Hopf, D.L. Kaplan, and R.L. Shoemaker, *Phys. Rev. Lett.* **46**, 474 (1981).
 - [4] H. Nakatsuka, S. Asaka, H. Itoh, K. Ikeda, and M. Matsuoka, *Phys. Rev. Lett.* **50**, 109 (1983); A.T. Rosenberger, L.A. Orozco, and H.J. Kimble, *Phys. Rev. A* **28**, 2569 (1983).
 - [5] R. Bonifacio and L.A. Lugiato, *Phys. Rev. Lett.* **40**, 1023 (1978); *Phys. Rev. A* **18**, 1129 (1978); *Lett. Nuovo Cimento* **21**, 505 (1978).

- [6] L Mandel and E. Wolf, *Optical Coherence and Quantum Optics*, (Cambridge University Press, Cambridge, 1995).
- [7] L.M. Narducci, R. Gilmore, D.H. Feng, G.S. Agarwal, *Opt. Lett.* **2**, 88 (1978).
- [8] M. Weidinger, B.T.H. Varcoe, R. Heerlein, H. Walther, *Phys. Rev. Lett.* **82**, 3796 (1999); B.T.H. Varcoe, S. Brattke, M. Weidinger, H. Walther, *Nature* **403**, 743 (2000).
- [9] S. Haroche, and J. M. Raimond, *Exploring the Quantum*, (Oxford University Press, Oxford, 2006).
- [10] C.J. Hood, T.W. Lynn, A.C. Doherty, A.S. Parkins, and H.J. Kimble, *Science* **287**, 1447 (2000); P.W. H. Pinkse, T. Fisher, P. Maunz, and G. Rempe, *Nature* **404**, 365 (2000).
- [11] P. Domokos and H. Ritsch, *Phys. Rev. Lett.* **89**, 253003 (2002); J.K. Asbóth, P. Domokos, H. Ritsch and A. Vukics, *Phys. Rev. A* **72**, 053417 (2005).
- [12] P. Domokos and H. Ritsch, *J. Opt. Soc. Am. B* **20**, 1098 (2003).
- [13] P. Maunz, T. Puppe, I. Schuster, N. Syassen, P.W.H. Pinkse, and G. Rempe, *Nature (London)* **428**, 50 (2004).
- [14] A.T. Black, H.W. Chan, and V. Vuletić, *Phys. Rev. Lett.* **91**, 203001 (2003).
- [15] B. Nagorny, T. Elsässer, and A. Hemmerich, *Phys. Rev. Lett.* **91**, 153003 (2003); D. Kruse, C. von Cube, C. Zimmermann, and P. W. Courteille, *Phys. Rev. Lett.* **91**, 183601 (2003).
- [16] S. Slama, G. Krentz, S. Bux, C. Zimmermann, P. W. Courteille, *Phys. Rev. A* **75**, 063620 (2007).
- [17] F. Brennecke, T. Donner, S. Ritter, T. Bourdel, M. Köhn, and T. Esslinger, *nature* **450**, 268 (2007).
- [18] P. Treutlein, D. Hunger, S. Camerer, T. W. Hänsch, and J. Reichel, *Phys. Rev. Lett.* **99**, 140403 (2007); Y. Colombe, T. Steinmetz, G. Dubois, F. Linke, D. Hunger, and J. Reichel, *Nature* **450**, 272 (2007).
- [19] S. Gupta, K. L. Moore, K. W. Murch, and D. M. Stamper-Kurn, *Phys. Rev. Lett.* **99**, 213601 (2007).
- [20] C. Maschler and H. Ritsch, *Phys. Rev. Lett.* **95**, 260401 (2005).
- [21] J. Larson, B. Damski, G. Morigi, and M. Lewenstein, *Phys. Rev. Lett.* **100**, 050401 (2008).
- [22] J. Larson, S. Fernandez-Vidal, G. Morigi, and M. Lewenstein, *New J. Phys.* **10**, 045002 (2008).
- [23] M. Lewenstein, A. Kubasiak, J. Larson, C. Menotti, G. Morigi, K. Osterloh, and A. Sanpera, in *Atom. Phys. 20, Proc. of ICAP 2006 Innsbruck*, AIP Conference Series **869**, C. Roos and H. Haefner, and R. Blatt (Eds.), (AIP, Melville, NY, 2006), p. 201.
- [24] C.W. Gardiner, and P. Zoller, *Quantum Noise*, (Springer-Verlag, Berlin, 2000).
- [25] S. Fernandez-Vidal, S. Zippilli and G. Morigi, *Phys. Rev. A* **76**, 053829 (2007).
- [26] N.W. Ashcroft and D. Mermin, *Solid State Physics*, (hardcourt Brace Collage Publishers, Forthworth TX, 1976).
- [27] X.-G. Wen *Quantum Field Theory of Many-Body Systems*, (Oxford University Press, Oxford, 2004).
- [28] In the strict graphene context, see for instance, K. S. Novoselov *et al.*, *Nature* **438**, 197 (2005); and for cold atoms context, S.-L. Zhu, B. Wang, and L.-M. Duan, *Phys. Rev. Lett.* **98**, 260402 (2007).
- [29] J. Larson and J.-P. Martikainen (unpublished).